Academic Journal of Science and Technology
ISSN: 2771-3032 | Vol. 2, No. 2, 2022

Effect of Bimetallic and Halogen Ions on Performance in Inorganic Double Perovskites

Xinlong Li[1], Suxian Fu[1], Mengyan Li[2], Kuan Cheng[1], Shujuan Xiao[1, *]

[1] College of Materials Science and Engineering, North China University of Science and Technology, Tangshan 06210, Hebei, China
[2] College of Clinical Medicine, North China University of Science and Technology, Tangshan 06210, Hebei, China

[*] **Corresponding author**: Shujuan Xiao (Email: xiaosj@ncst.edu.cn)

Abstract: In the context of low-carbon environmental protection, the de-leading of perovskite materials has become a hot spot in research, and replacing the position of lead in perovskites with suitable low-toxic elements is particularly important for improving the toxicity of perovskites. The proposal of all-inorganic bimetallic perovskites provides a new direction for the crystal structure composition of perovskites, and the substitution of lead ions by bimetallic ions greatly reduces the toxicity of perovskites and improves the stability of the material. However, new problems have also arisen, bimetallic perovskites have indirect band gaps will reduce the optical properties of perovskites, adjusting the band gap of compounds has become the main problem in the study of bimetallic perovskites, this paper reviews the impact of adjusting different B-bit ions and X-bit halogen ions on the performance of perovskites, and makes an outlook on the development prospects of perovskites.

Keywords: Band gap, De-leaded, Inorganic bimetallic perovskites.

1. Introduction

In recent years, oil and coal resources have been greatly consumed, people urgently need new energy to replace these non-renewable energy sources. In this context, the use of solar energy has achieved unprecedented development, and the development of materials that can transform solar energy into chemical energy has become the goal of many researchers. Perovskite materials, as the third generation of new semiconductor materials, have attracted people's attention and have been widely used in solar cells, photodetectors [1-5] and other optoelectronic devices due to their excellent material characteristics [6-10], such as adjustable band gap, high carrier migration rate, low defect density and high-power conversion efficiency (PCE). As the most likely replacement of silicon in the new photoelectric materials.

In the development of perovskite materials, three-dimensional perovskites were first developed, taking lead-based three-dimensional perovskite $APbX_3$ as an example, where A is a methyl ammonium ion (or formamide ion) and X is a halogen ion (Cl^-, Br^-, I^-). Since Kojima A [11] first measured the PCE of $MAPbX_3$ dye-sensitized batteries at 3.81% in experiments (the highest when the X-ion was I-highest), the PCE of organohalide perovskites has reached 29.8% (certified by the National Renewable Energy Laboratory of the United States) [12]. Although the organic halide perovskite has achieved such a high photoelectric conversion efficiency, it has not yet been vigorously promoted by the market, mainly because of the poor stability of such perovskites and the content of heavy metal ion lead. Taking $CH_3NH_3PbI_3$ as an example, the synthesis reaction equation is:

$$PbI_2 + CH_3NH_3I \leftrightarrows CH_3NH_3PbI_3 \quad (1)$$

In some environments (oxygen-rich, humid, UV irradiation, etc.), lead methyl ammonium iodide breaks down into CH_3NH_3I and PbI_2 or directly degrades into other chemicals. A similar decomposition reaction occurs when the X-ion is Br^-, Cl^-, or is itself a mixture of halide perovskites [13]. In order to solve this problem, the researchers tried to replace organic cations with metal ions (Cs^{2+}, Rb^{2+}), first of all, through the tolerance factor t to assess whether the A-position ion can stabilize the BX_3 octahedral structure (when $0.8 \leqslant t \leqslant 1$, perovskite will form; $t>1$,A-position ion is too large to form 3D perovskite; $t<0.8$, will form a non-perovskite structure.)

$$t = \frac{R_A + R_X}{\sqrt{2(R_B + R_X)}} \quad (2)$$

R_A: A-site ion radius; R_B: B-site ion radius; R_X: X-site ion radius

In order to make the tolerance factor $t \approx 1$, the A-bit ion radius is much larger than the B-bit ion radius, so Cs^{2+} is most suitable as an A-bit ion. However, the radius of Cs^{2+} still does not meet the stability requirements, and the stability of perovskites will be maintained by using halogen atoms with larger radii [14]. This all-inorganic perovskite has better stability than devices made of organic perovskites and organic-inorganic hybrid perovskites.

In order to solve the lead toxicity of perovskite materials, replacing lead ions with non-toxic metal ions is the mainstream of today's perovskite development [15-16], such as the IVA group elements Ge^{2+} and Sn^{2+} replacing Pb^{2+}, and the three elements are located in the same main group with similar electronic arrangement. In 2014, Hao Feng [17] first reported $CH_3NH_3SnI_3$ perovskite with an optical bandgap of 1.3 eV, with an initial power conversion efficiency of 5.73%, the amount of halogen ions in $CH_3NH_3SnI_xBr_{3-x}$ adjusted by band gap engineering, which can control the coverage of most of the visible spectrum, and regulate the performance of the battery by changing the ratio of Sn and Pb, the data show that when X=0.5, the material has a wider light absorption and the highest short-circuit photocurrent density of 20 Ma cm^{-2} (obtained at 100 mW cm^{-2} simulated full daylight conditions).

Although Ge^{2+} and Sn^{2+} ions can improve the toxicity of perovskites, their stability is poor and it is difficult to get out

of the laboratory. Taking $MASnI_3$ as an example, Sn^{2+} is easily oxidized to Sn^{4+} (the 5s orbit of Sn^{2+} makes perovskites easy to be oxidized) Perovskites are rapidly degraded to produce higher carrier density and conductivity, and then the device will be short-circuited. Compared with Sn^{2+}, Ge^{2+} has less application in perovskite materials, mainly due to the high cost.

In recent years, the application of plasma ion substitution to B-bit ions has been widely recognized by researchers, and inorganic B-bit bimetallic halide perovskites stand out with their low toxicity and excellent stability [18]. This type of perovskite can be roughly divided into two types of $A_2B(I)B(III)X_6$ and $A_2B(II)B(II)X_6$ according to the valence state of B-bit ions. In 2016, Eric T [19] reported that $Cs_2AgBiBr_6$ and $Cs_2AgBiCl_6$ were synthesized by solid-state and solution routes, and their bandgap widths of 2.19 eV and 2.77 eV were measured, which were slightly smaller than $CH_3NH_3PbBr_3$ with a bandgap width of 2.26 eV and $CH_3NH_3PbCl_3$ at 3.00 eV. As can be seen in Figure 1, the top of the valence band of both is mainly composed of the orbitals of halogen ions, and the bottom of the conduction band is mainly composed of the orbitals of Bi ions, and when the electrons jump from the top of the valence band to the bottom of the conduction band, the electrons may transition from the p-orbital of the halogen ions to the p-orbital of the Bi ions. Therefore, one of the reasons why the band gap of $Cs_2AgBiCl_6$ is greater than that of $Cs_2AgBiBr_6$ may be that the attraction of the Cl consideration electron is stronger than that of the Br consideration electron, because the former has large electronegativity and small radius, so the electron is not easy to detach (small electronegativity, narrow band gap). However, they are less stable and degrade within weeks under air and light conditions.

Like many types of perovskites, inorganic bimetallic perovskites are also qualified in the photovoltaic field (as shown in Figure 2). Thanks to the durability of the material itself and the low cost of synthesis, inorganic double perovskites have received widespread attention in recent years. In this paper, the effects of different B-site bimetallic ion combinations and different halogen atoms on the properties of perovskites are explored through the crystal structure and electronic structure of such inorganic bimetallic perovskites.

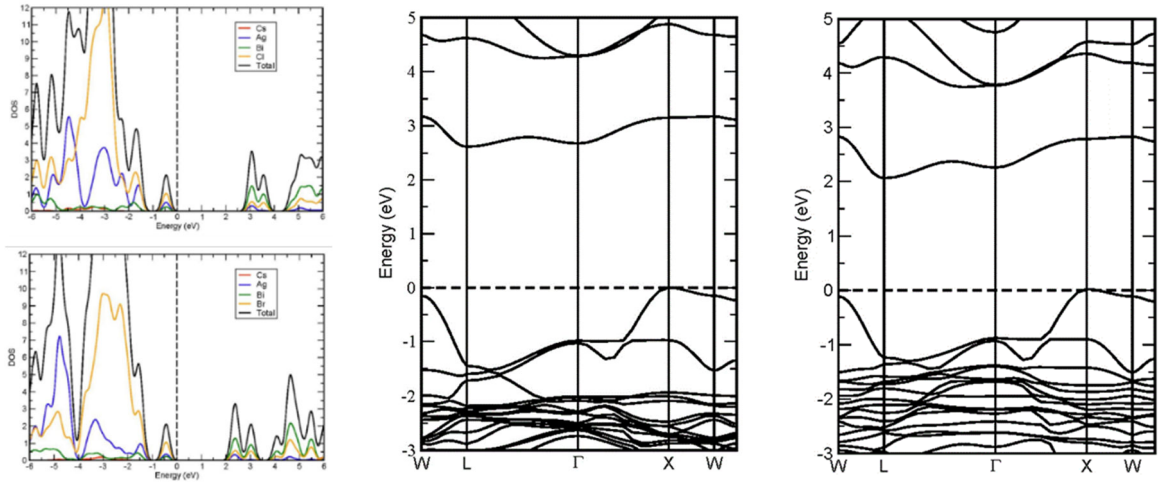

(a) (b) (c)

Figure 1. a. Atomic partial density of states maps for $Cs_2AgBiCl_6$ (top) and $Cs_2AgBiBr_6$ (bottom). b. Band structure diagrams for $Cs_2AgBiCl_6$. c. Band structure diagrams for $Cs_2AgBiBr_6$. (The Fermi energy is set to E = 0 and denoted with a dashed line) [19].

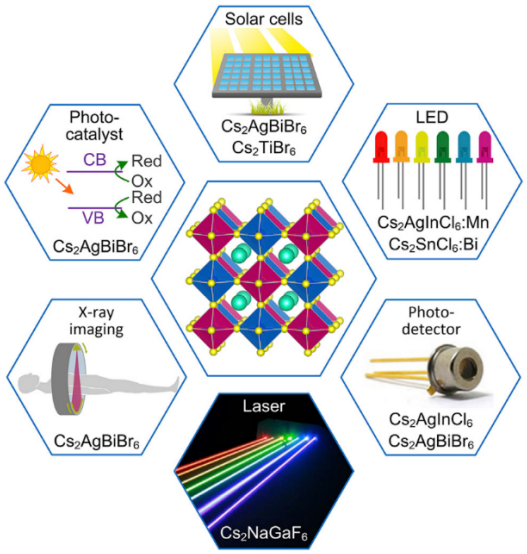

Figure 2. Current and potential applications of halide double perovskites. (For each application, the chemical formula of representative halide double perovskites is given) [20].

2. Effect of Bimetallic Ions on The Properties of Perovskites

2.1. $A_2B(I)B(III)X_6$ Perovskite

Theoretical studies have shown that the main factor determining the photoelectric properties of halide lead-based perovskites is the $6s^2$ solitary pair of electrons and inactive 6p orbitals of Pb^{2+}. When B-bit ions are +1 valence and +3 valence, such perovskites can be divided into three subgroups by the presence of solitary electron pairs of B-bit ions: B(I) and B(III) ions both contain solitary pair electrons; Only one of the B(I) and B(III) ions contains solitary pairs of electrons; Neither the B(I) nor B(III) ions contain solitary pairs of electrons [21].

2.1.1. Both B-site Double Ions Contain Lone Electron Pairs

$Cs_2InBiCl_6$ as a representative of the first type of double perovskites (as of now, it has not been synthesized in experiments), but Saeed [22] used density functional theory to study the structural geometry, electron band gap, state density of Cs_2InBiX_6 (X=F, Cl, Br, I), confirming that the valence band is mainly composed of ins orbitals, the conduction band is mainly composed of Bi's p-orbital, and the mechanical properties show that Cs_2InBiX_6 (X=F, Cl, Br, Br, etc.) is confirmed that the valence band is mainly composed of ins orbitals of In, the conductive band is mainly composed of the p-orbital of Bi, and the mechanical properties show that Cs_2InBiX_6 (X=F, Cl, Br, I) Meet the stability standards of the cubic structure and achieve optical characteristics comparable to $MAPbI_3$. In 2016, Deng [23] reported that $(MA)_2TlBiBr_6$ is the only perovskite that has been successfully synthesized so far, both B(I) and B(III) ions, but Tl is more toxic than Pb.

2.1.2. The B-site Double Ion Contains A Lone Electron Pair

The second class of inorganic biperovskite B(I) ions are generally Na^+, K^+, Rb^+, Ag^+, Cu^+, B(III) is Bi^{3+}, the conduction band of such compounds is composed of the p-orbital of Bi, and the valence band is composed of the 6s orbital of Bi and the p-orbital of halogen ions. This composition causes perovskites to produce a large band gap (>3 eV), if such perovskites are applied to solar cells, the adjustment of the band gap will be the primary problem to be solved, and the band gap must be controlled in the range that can effectively absorb visible light. Slavney [24] added CsBr, AgBr, and $BiBr_3$ to HBr solution to cultivate $Cs_2AgBiBr_6$ single crystals, which made a major breakthrough in device lifetime by measuring an indoor luminescence lifetime of about 660 ns, much higher than the (MA) $PbBr_3$ film luminescence lifetime of 170 ns [25], and approaching the lifetime of the optimized (MA)$PbBr_3$ film of 736ns-1μs [26,27]. But these perovskites have indirect band gaps, and PCE is lower in single junction solar cells. Hu [28] used first principles to study the structure, electrons and other properties of Cs_2CuBiX_6 (X=I, Br, Cl) perovskites, and measured that Cs_2CuBiX_6 (X=I, Br, Cl) were indirect bandgap semiconductors, and the band gap values of Cs_2CuBiX_6 (X=I, Br, Cl) were 0.78 eV, 1.13 eV and 1.29 eV, respectively, and the crystal structure was optimized by using the PBE-GGA function, and the lattice parameters were shown in Table 1. The lattice parameters and volume are gradually decreasing, and the data are in line with Nabi's report [29] $Cs_2CuBiCl_6$ with a lattice constant of 10.64 Å. By calculating that the negative binding energy (E_b) and formation energy (E_f) of the compound are less than zero, the thermodynamic stability and synthesis feasibility of the compound are proved.

Table 1. Lattice parameters, Goldsmith's tolerance factor (t_G), binding energies (E_b) and formation energies (E_f) of double perovskites Cs_2CuBiX_6 (X=I, Br, Cl) [28].

Compounds	a=b=c(Å)	V (Å^3)	t_G	E_b	E_f	Ref.
Cs_2CuBiI_6	12.00	1728.00	0.88	-2.7215	-1.2829	[28]
$Cs_2CuBiBr_6$	11.19	1401.17	0.90	-3.0787	-1.9879	[28]
	10.895					[30]
$C_sCuBiCl_6$	10.64	1204.55	0.91	-3.4112	-2.3840	[28]
	10.64	1079.05				[29]
	10.366					[30]

2.1.3. None of the B-site Ions Contain Solitary Electron Pairs

There are many types of the third type of inorganic double perovskites, and most of the +1 valent cations applicable to the B-bit ions of perovskites do not contain solitary pairs of electrons. However, among all the compounds, only Ag^+ and Cu^+, which occupy state d^{10}, and In^{3+} and TI^{3+} that occupy state s^0, will have small band gaps. In 2018, Locardi [31] reported for the first time the synthesis of $Cs_2AgInCl_6$, and the optical properties and size distribution of materials were regulated by doped Mn^{2+}, and the photoluminescent quantum yield (PLQY) increased from 1.6% to 16%. Since the electron is excited, it is the transition from halogen ions to B-site ions, because Mn's atomic orbitals are lower than the energy of In and Ag, so the band gap after incorporation of Mn^{2+} is reduced. In addition, the 3D orbital of the Mn ion is in a semi-full state, so its energy will be further reduced. The structural model is shown in Figure 3.

Cs_2NaGaF_6 also falls into the third category, with Wang [33] studying Cs_2NaGaF_6 single crystals by X-ray diffraction and polarization Raman scattering, which has a hexagonal structure symmetrical $R\bar{3}m$（D_{3d}^5）and a skeleton consisting of GaF_6 octahedrons connected to each other by NaF_6 octahedrons shared by faces and horns. As shown in Figure 4, this perovskite structure consists of 12 layers of Ga^+ and Na^+ stacked along the C axis, so it is considered a "12-L type".

In all-inorganic double perovskites, A-bit ions are identified as metal (or inorganic) cations, such as Cs^+, Rb^+, and Na^+, etc. The B-bit ions are replaced by Pb^{2+} into two metal ions with different valence states. According to the atomic orbitals of B-bit ions, such $A_2B(I)B(III)X_6$ perovskites are divided into four categories [34], as shown in Table 2.

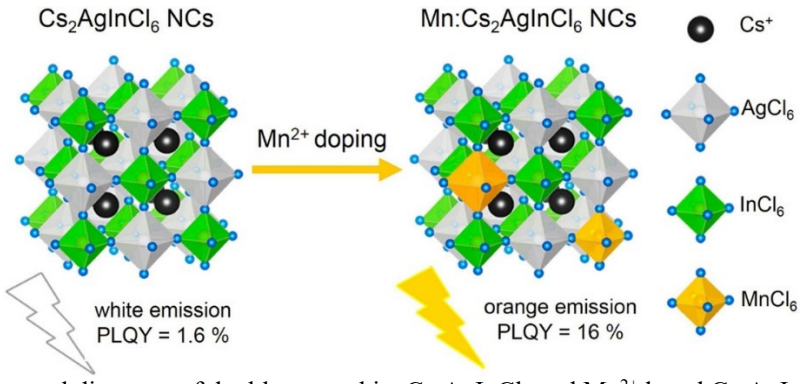

Figure 3. Structural diagrams of double perovskite $Cs_2AgInCl_6$ and Mn^{2+}doped $Cs_2AgInCl_6$ NCs [32].

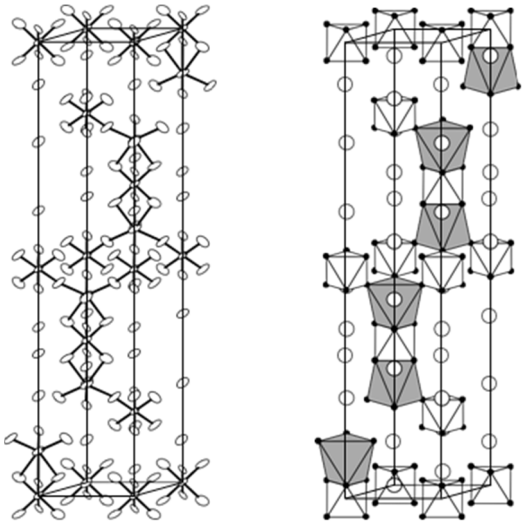

Figure 4. An Ortep view (left) and a polyhedral representation (right) from the neutron refinement showing the connectivity between the GaF_6 and the NaF_6 octahedra. The white and grey polyhedral represent GaF_6 and NaF_6, respectively, while the white and black atoms correspond to Ce and F [33].

Table 2. All-inorganic double perovskite classification [34].

Type	Atomic orbitals	Element	Peculiarity
Alkali metals/nitrogen group elements	$3s^1$,$4s^1$/$6s^2$,$5s^2$	B(I)=Na^+ and K^+/ B(III)=Bi^{3+} and Sb^{3+}	Partially synthesizable, the optical performance is not good
Post-transition metal/nitrogen group elements	$6s^2$,$5s^2$/$6s^2$,$5s^2$	B(I)=TI^+ and In^+/ B(III)= Bi^{3+} and Sb^{3+}	The band gap is small, the performance is good, but it is difficult to synthesize
Precious metals/post-excessive	$4d^{10}$/$5s^2$,$4s^2$	B(I)=Cu^+ and Ag^+/ B(III)=In^{3+} and Ga^{3+}	Partially synthesizable, the optical performance is not good
Precious metals/nitrogen group elements	$4d^{10}$/$6s^2$,$5s^2$	B(I)= Cu^+,Ag^+ and Au^+ B(III)= Bi^{3+} and Sb^{3+}	Partially synthesizable, the optical performance is not good

2.2. $A_2B(II)B(II)X_6$ Perovskite

Compared with $A_2B(I)B(III)X_6$ perovskites, the number of $A_2B(II)B(II)X_6$ perovskites has been reported to be very small, and most of them are limited to theoretical research.

Gao [35] applied the EXtreme Gradient Boosting Regression (XGBR) algorithm to a robust and predictable machine learning model (ML) for perovskite materials to obtain two novel lead-free inorganic double perovskites Na2MgMnI6 (direct band gap of 1.89 eV) and K_2NaInI_6 (direct band gap of 1.46 eV) similar to organic-inorganic perovskites ($MAPI_3$) $CH_3NH_3PbI_3$ (E_g = 1.6 eV), the valence band top is mainly composed of the p-orbital of X-bit ions, the conduction band bottom of K_2NaInI_6 is mainly composed of X-bit ions, and the conduction band bottom of Na_2MgMnI_6 is mainly composed of B-bit ions, and the band structure and projection density of the two perovskites are shown in Figure 5. With T. Compared with the conduction band bottom of $Cs_2AgInCl_6$ perovskite synthesized by Thao Tran [36] (composed of In's 5s orbital), the difference in crystal composition is that the halogen ions are Cl^- and I^-, and the monovalent ions are Ag^+ and Na^+. The difference in the bottom composition of the conduction band may be due to the

fact that the two monovalent ions of the crystal have only s orbitals in the ground state, while the Ag ions have d orbitals, and the halogen ions can coordinate with Ag and In, while the K_2NaInI_6 crystal can only coordinate with In, and the Cl electronegativity is high, and it is less likely to obtain another electron than the I ion after obtaining the electron.

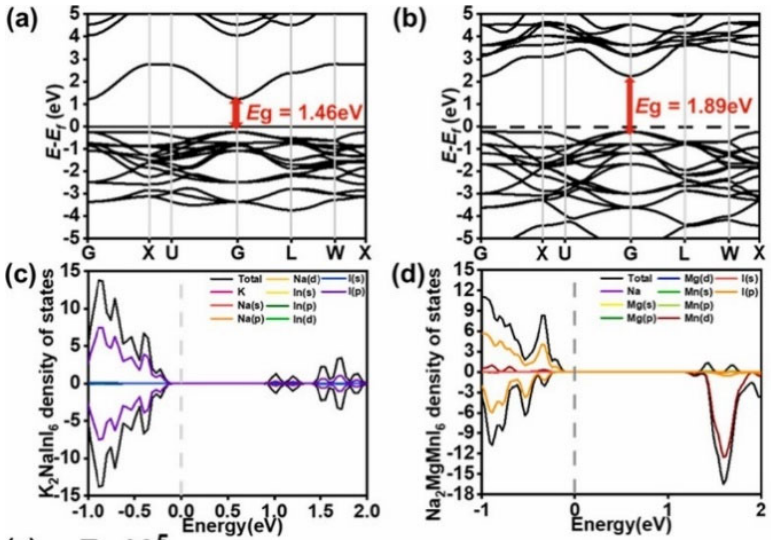

Figure 5. a is the electronic band structure of K_2NaInI_6, the right is the electronic energy band structure of Na_2MgMnI_6, c is the projected density of states (PDOS) of K_2NaInI_6, and d is the projected density of states (PDOS) of Na_2MgMnI_6 [36].

3. Effect of Halogen Atoms on The Properties of Perovskites

Adjusting the properties of perovskites by changing the type of halogen atom or changing the amount of halogen atoms in the compound is an effective way to adjust the properties of perovskites. The same type of perovskite composed of different types (or different contents) of halogen atoms may differ in material stability, material band gap, carrier transport capacity, device life, etc. This section describes the effects of different kinds (or content) of halogen atoms on the properties of perovskite.

3.1. Single Halogen Double Perovskites

The most common and simplest method is to achieve suitable band gap and material stability by replacing different halogen atoms. Changes in halogens do not redefine perovskites, but preserve some of the properties of the metal ions at the A and B levels of the perovskite compound. Researchers generally take the substitution between X=F, Cl, Br, and I.

Saba Iqbal [37] report that the photoelectric and thermoelectric properties of Rb_2AlInX_6 (X=Cl, Br, I) were studied using the DFT algorithm, and the crystal structure is shown in Figure 6a. Most halogen bimetallic perovskites are cubic crystalline systems and belong to the $Fm\bar{3}m$ dot group.

By looking at the PDOS image in Figure 6c, the conduction band bottom of the three compounds is composed of a 3p orbital of Al and a small amount of In's 5p orbital, and when the X-ion is Cl, the PDOS peak is more concentrated and biased towards high energy, while from Br to I, PDOS gradually flattens and moves in the direction of low energy. Of course, not only Al ions, but also PDOS of other ions have such phenomena, although the orbits that make up the valence band are moving from low energy to high energy, but the PDOS image does not change from concentration to flatness, but compresses in the y-axis direction. Therefore, the band gap shown in the energy band structure diagram gradually becomes smaller, the shape of each energy band is roughly unchanged, the lower valence band moves up to the top of the valence band, and the upper guide band moves down. The bottom energy of the valence band shifts up because compared to Cl, I^- has a large ion radius, small electronegativity, and easy to lose electrons. However, its orbit is extremely similar, so the PDOS shape remains roughly unchanged. Since the 5p orbital of In in the valence band may not have a large interaction with the X-ion, the approximate shape is not affected by the X-ion. The orbit of the conduction band is different from the valence band orbital, and the electron has to transition from the halogen to the orbit of the metal ion, so the orbital of the halogen may have a greater effect on the orbit of the metal in the conduction band. As the electronegativity of halogen atoms decreases, the orbitals of metal ions are constrained less.

Zhang [38] reported the high-voltage regulation of the optical properties of $Cs_2AgBiCl_6$ crystals in the paper, and analyzed two halogen perovskite materials in terms of morphological characteristics, ultraviolet absorbable spectroscopy experiments, X-ray diffraction experiments, and in situ high-pressure Raman spectroscopy. Fu Ruijing [39] reported that $Cs_2AgBiBr_6$ was analyzed using the same method, and now compares the experimental results of the two:

To determine how the band gap of $Cs_2AgBiCl_6$ varies with compression, Zhang performed in situ high-pressure UV-vis absorption measurements up to 31 GPa (Figure 7a). $Cs_2AgBiCl_6$ shows a sharp increase in absorption below 440 nm, with mild absorption trailing under environmental conditions, indicating an indirect band gap feature, which is substantially consistent with the findings of the study of G Volonakis [40]. The band gap of $Cs_2AgBiCl_6$ is extrapolated $(\alpha dh\nu)^{1/2}$ with hν in the indirect band gap Tauc diagram (where α is the absorption coefficient, d is the sample thickness, and hν is the photon energy) as shown in Figure 7b, with the indirect band gap reaching 2.84eV. Pressure-driven bandgap evolution of $Cs_2AgBiCl_6$ after compression is shown in Figure 7c. As the pressure increases, the band gap of $Cs_2AgBiCl_6$ gradually redshifts below 5GPa, followed by a

sharp increase above 5GPa in the small pressure region. As the pressure increases further above 7 GPa, a redshift in the band gap is observed. When the applied pressure reaches approximately 14GPa, the band gap remains largely stable. During decompression, the absorption spectrum of $Cs_2AgBiCl_6$ remains blueshipped above 0.8GPa.

Fu used of high-voltage ADXRD spectra and in situ high-pressure Ramanpu in his studies also confirmed red-blueshift changes in the absorption spectrum, and that there was a cubic-to-quadrangular phase transition in $Cs_2AgBiCl_6$ throughout the pressurization process. However, after the pressure is released, the structure of the perovskite is a mixture of cubic and tetragonal phases, which causes the band gap value after decompression to be greater than the initial value. An image of the change of band gap with pressure of $Cs_2AgBiCl_6$ is shown in Figure 8b, and for cubic structures, the band gap decreases as the pressure increases. In Fig. 9 and Figure 10, the energy band structure diagram of the cubic phase and the quadrilateral phase at four pressures is shown, respectively, and the $Cs_2AgBiCl_6$ of the cubic phase gradually decreases with the increase of pressure; For $Cs_2AgBiCl_6$ in the quadrilateral phase, when the pressure increases, the band gap will produce an inflection point to increase the band gap during the gradual reduction process, which is also consistent with the conclusion of Figure 7c.

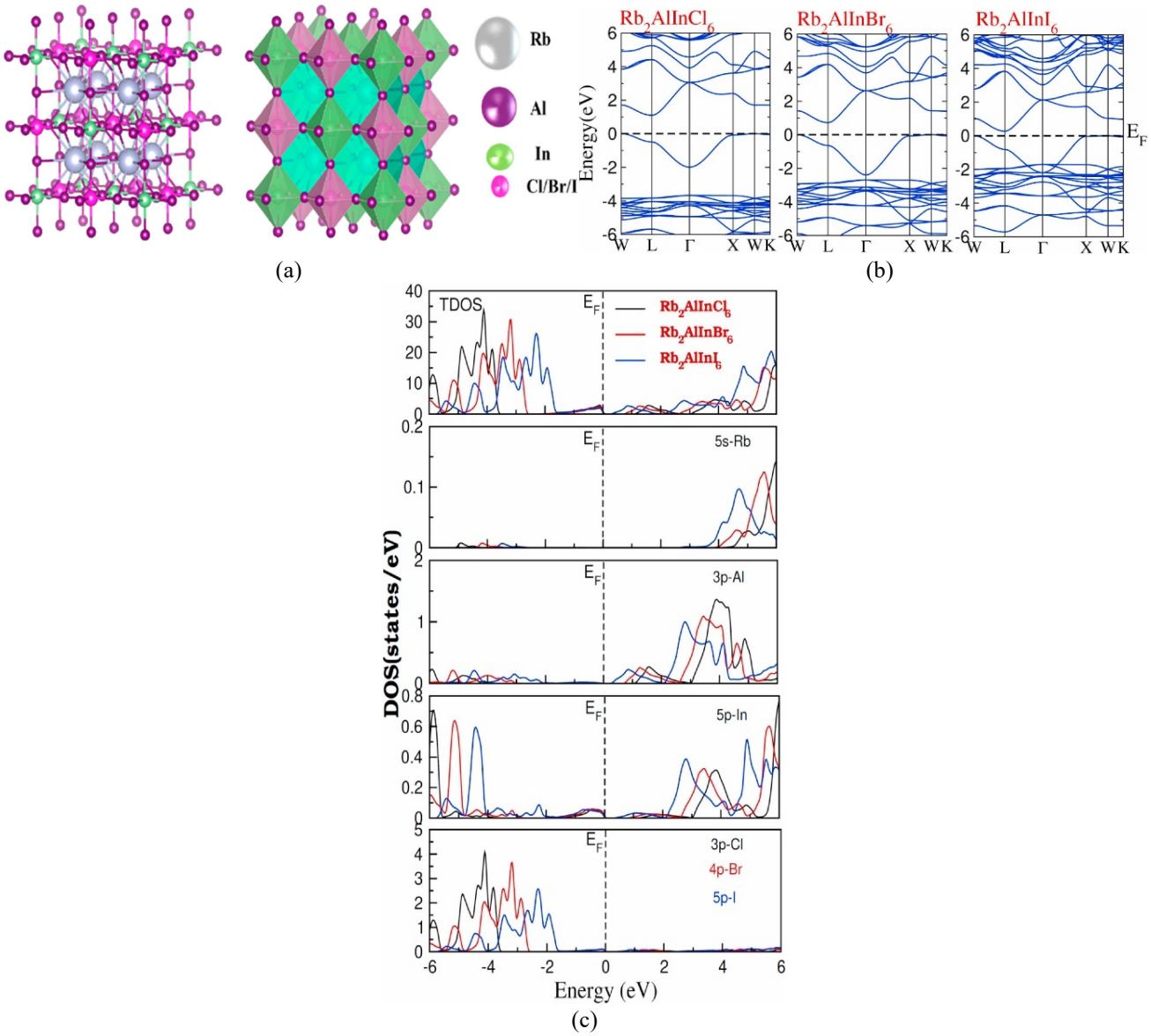

Figure 6. a. Cubic unit cell of the double perovskite Rb_2AlInX_6 (X = Cl, Br and I) in atomic form (left) and polyhedral form (right). Grey balls represent Rb atoms, purple balls represent Al atoms, and green and pink balls represent Al and Cl/Br/I atoms. b. Rb_2AlInX_6 (X = Cl, Br, I) electronic band structure. c. Calculated total (TDOS) of $Rb_2AlInCl/Br/I_6$ as well as PDOS of Al atom, In atom as well as X atom by TB-mBJ potential [37].

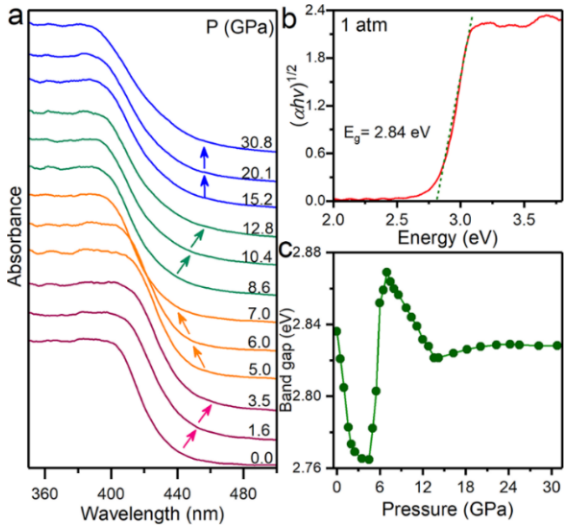

Figure 6 .(a) Absorption spectra of $Cs_2AgBiCl_6$ as a function of (a) Absorption spectra of $Cs_2AgBiCl_6$ as a function of pressure. The arrows trace the evolution of the absorption edge. (b) Indirect band gap Tauc plot for $Cs_2AgBiCl_6$ at ambient pressure. (c) Band gap evolution of $Cs_2AgBiCl_6$ as a function of pressure [38].

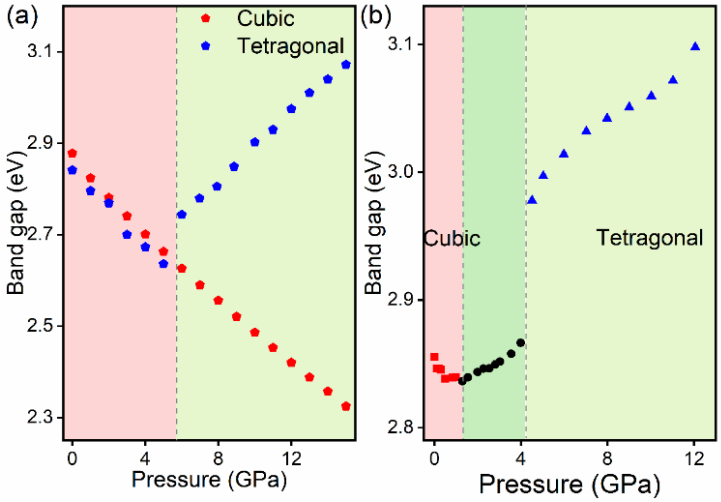

Figure 7. (a) $Cs_2AgBiBr_6$ cubic (red) and tetragonal (blue) band gap values as a function of pressure. (b) Band gap value of $Cs_2AgBiBr_6$ as a function of pressure [39].

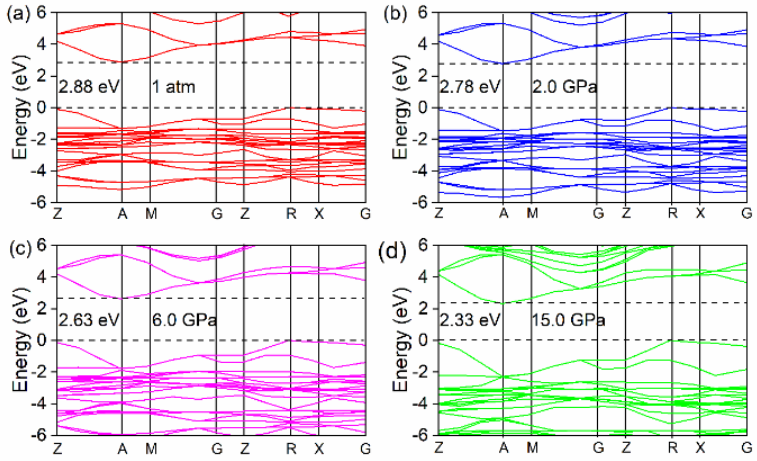

Figure 8. Theoretical calculated electronic band structures of the cubic phase $Cs_2AgBiBr_6$ at (a) 1 atm, (b) 2.0 GPa, (c) 6.0 GPa and (d) 15.0 GPa [39].

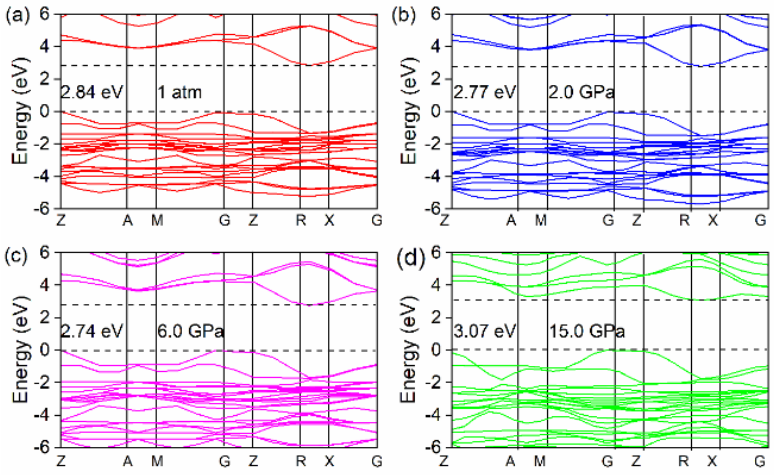

Figure 9. Theoretical calculated electronic band structures of the tetragonal $Cs_2AgBiBr_6$ at (a) 1 atm, (b) 2.0 GPa, (c) 6.0 GPa and (d) 15.0 GPa [39].

3.2. Mixed Halogen Fully Inorganic Double Perovskites

Compared with single halogen inorganic double perovskites, the method of mixing halogens can also achieve the purpose of adjusting band gap and performance. This method has been used in lead-based organic-inorganic hybrid perovskites [41,42]. However, mixed halogens are easy to make perovskite materials produce halogen separation under light conditions, and this photophasic separation effect limits the application of perovskites in solar cells and light-emitting diodes, while all-inorganic dipertenites will improve the photostability of the compound [43], and large-radius A-site cations play a crucial role in the stability of the material. However, the band gap of all-inorganic double perovskites is often relatively large, and the role played by changing the single halogen atom in adjusting the band gap has certain limitations, and changing the mixed halogen content provides more directions for everyone in adjusting the band gap of the material.

Han [44] reported on the study of mixed B-ions and mixed halogen-ion perovskites, systematically studied the electronic characteristics of mixed B-ions and X-ions in Cs2AgBiX6 perovskites through first-principles calculations, and found that the electron and hole life of mixed halogen double perovskites was significantly higher than that of bimetallic perovskites mixed with B-ions. Unlike B(I) and B(III) cation-bit alloys, $Cs_2AgBi(Br_xCl_{1-x})_6$ shows the virtual crystal behavior of VB and CB, as shown in Figure 11. The VB and CB of Cs_2AgBi $(Br_xCl_{1-x})_6$ are located between the energies of Cs2AgBiBr6 and $Cs_2AgBiCl_6$. This phenomenon is due to the small chemical differences between Cl and Br. At the same time, both VB and CB of $Cs_2AgBi(Br_xCl_{1-x})_6$ showed little broadening, which also showed that displacement disorder had little effect on the lifetime of the electronic state in $Cs_2AgBi(Br_xCl_{1-x})_6$.

4. Conclusion

Most inorganic bimetallic perovskites are group of $Fm\bar{3}m$ points when performing theoretical calculations, so when optimizing their geometry, they can be accelerated by their symmetry; The top of the valence band is generally composed of the p-orbital of the X-site ion, and the bottom of the conduction band is generally mainly composed of the lowest-energy atomic orbital of the B-site ion; The smaller the electronegativity of the atom at the top of the contribution valence band, the higher the energy of the valence band, the greater the electronegativity of the atom contributing to the bottom of the conduction band, the lower the conduction band energy, and the smaller the band gap; Between B-site ions and B-site ions, and between B-bit ions and X-site ions, the more the orbital energy matches, the lower the band gap; Elements with similar energy levels and structures constitute energy bands with similar shapes, such as changing the type of halogen atoms, which have less effect on the approximate shape of the energy bands; A-site ions do not contribute to the composition of the energy band, but only play a role in filling vacancies, balancing charge and stabilizing structure.

There are many ways to adjust the band gap of materials: dimensional reduction [45], molecular engineering [46], phase transitions [47], pressure regulation [39], strain modulation [48] etc. Perovskite materials because of their own special structure and properties, is a new star in the field of photovoltaics, many researchers have also invested in the study of perovskite, perovskite performance will also be further improved.

Acknowledgment

This work is supported by Innovation and Entrepreneurship Training Program for College Students of China. (NO. X2021032)

References

[1] Yaopanpan, Wanglingrui, Wangjiaxiang, et al. “Structural and optical properties of non-leaded diperovskite Cs_2TeCl_6 under high pressure [J],” Acta Physica Sinica, 2020,69(21):187-193.

[2] Jinshengli, Shouchuihui, Huangmianji, et al. “Research progress on the stability of perovskite solar cells and the trend of module industrialization [J],” Materials Reports, 2023(05).

[3] Duanjiashun, Pengliping, Yuhuayang, et al. “Research progress on the stability and efficiency of two-dimensional halide perovskite solar cells [J], ” Acta Materiae Compositae Sinica, 2022,39(05):1890-1906.

[4] Guowuqian, Chenhuaixi, Liuxitao, et al. “Rational assembly of mixed cation-enhanced metal halide perovskite crystal array photoelectric detection performance [J],” Science China Materials, 2022,65(01):179-185.

[5] Xinxing, “Progress has been made in the research of photoelectric detection crystal materials with rapid response from Fujian Institute of Physical Structure [J],” New Chemical Materials, 2018,46(08):292.

[6] Zhangyunxia, “Study on single crystal growth of organic-inorganic perovskites with band gap tunable and its photoelectric properties [D],” Shaanxi Normal University,2017.

[7] Mengguanghao, “ Study on the anisotropy of ultra-long exciton life and carrier mobility of new perovskite materials [D],” Dalian University of Technology,2018.

[8] Wangwanhai, Zhoujie, Tangweihua,“Application of perovskite film defect regulation strategy in solar cell [J],” Journal of Inorganic Materials,2022,37(02):129-139.

[9] Zhanghuanghu, Huangxin, “Trans perovskite batteries break world records in efficiency [N],” China Science Daily,2022-02-16(003).

[10] Yichenyi, “High performance perovskite solar cells [C],” 2017 Special Conference on Energy Storage Materials and Energy Conversion Technology,2017:16.

[11] Kojima A, Teshima K, Shirai Y, et al. “Organometal halide perovskites as visible-light sensitizers for photovoltaic cells[J],” Journal of the american chemical society, 2009, 131(17): 6050-6051.

[12] “National Renewable Energy Laboratory (NREL), Best Research Efficiencies Chart,” https://www.nrel.gov/pv/cell-efficiency.html, Accessed 2020-2.

[13] Niu G, Guo X, Wang L. “Review of recent progress in chemical stability of perovskite solar cells[J], ” Journal of Materials Chemistry A, 2015, 3(17): 8970-8980.

[14] Huangyang, Sunqingde, Xuwe, et al. “Advances in the theoretical research of materials for halogenated perovskite solar cells[J],” Acta Physico-Chimica Sinica,2017,33(09):1730-1751.

[15] Zhangjing, Sunhongrui, Ganxinlei, et al. “Lead reduction and stability study of inorganic perovskite solar cells[C],” Proceedings of the 7th Symposium on Materials Science and Technology for Novel Solar Cells,2020:222.

[16] Limeng, “Research on efficient and stable perovskite solar cells [D],” Soochow University,2018.

[17] Hao F, Stoumpos C C, Cao D H, et al. “Lead-free solid-state organic–inorganic halide perovskite solar cells[J],” Nature photonics, 2014, 8(6): 489-494.

[18] Huangqihang, Sunxiaoqin, “Photocatalytic water decomposition of transition metal-doped diperovskite Ba2InNbO6[J], ” Chemistry,2021,84(11):1231-1236.

[19] McClure E T, Ball M R, Windl W, et al. “ Cs_2AgBiX_6 (X= Br, Cl): new visible light absorbing, lead-free halide perovskite semiconductors[J],” Chemistry of Materials, 2016, 28(5): 1348-1354.

[20] Zhao X G, Yang D, Ren J C, et al. “Rational design of halide double perovskites for optoelectronic applications[J],” Joule, 2018, 2(9): 1662-1673.

[21] Zhaodianlong, Litianshu, Xuqiaoling , et al. “Research progress on the optimal design of halide perovskite photovoltaic materials[J],” Chinese Optics,2019,12(05):964-992.

[22] Muhammad Saeed, Izaz Ul Haq, Shafiq Ur Rehman, et al. “Imad Khan.Optoelectronic and elastic properties of metal halides double perovskites Cs_2InBiX_6(X = F, Cl, Br, I)[J],” Chinese Optics Letters,2021,19(03):21-30.

[23] Deng, Zeyu ,et al. “ Exploring the properties of lead-free hybrid double perovskites using a combined computational-experimental approach[J], ” Journal of Materials Chemistry, A. Materials for energy and sustainability, 2016,4(31):12025-12029.

[24] Slavney Adam H, et al. “A Bismuth-Halide Double Perovskite with Long Carrier Recombination Lifetime for Photovoltaic Applications.[J] ,” Journal of the American Chemical Society, 2016, 138(7) : 2138-41.

[25] Shi Dong, et al. “Low trap-state density and long carrier diffusion in organolead trihalide perovskite single crystals[J] ,” Science, 2015, 347(6221) : 519-522.

[26] Zhou H, Chen Q, Li G, et al. “ Interface engineering of highly efficient perovskite solar cells[J] ,” Science, 2014, 345(6196): 542-546.

[27] De Quilettes D W, Vorpahl S M, Stranks S D, et al. “Impact of microstructure on local carrier lifetime in perovskite solar cells[J] ,” Science, 2015, 348(6235): 683-686.

[28] Hu De-Yuan, et al. “First-principles study on the structural, elastic, electronic and optical properties of lead-free double perovskites Cs_2CuBiX_6 (X=I, Br, Cl)[J] ,” Materials Today Communications, 2021, 29.

[29] Nabi M, Gupta D C. “New Lead Free Halide Double Perovskite Materials: Potential Substitutes Towards Green Technology and Stable Optoelectronic Application[J] ,”2021.

[30] Feng H J, Deng W, Yang K, et al. “Double perovskite Cs_2BBiX_6 (B= Ag, Cu; X= Br, Cl)/TiO_2 heterojunction: an efficient Pb-free perovskite interface for charge extraction[J] ,” The Journal of Physical Chemistry C, 2017, 121(8): 4471-4480.

[31] Locardi F, Cirignano M, Baranov D, et al. “Colloidal synthesis of double perovskite $Cs_2AgInCl_6$ and Mn-doped $Cs_2AgInCl_6$ nanocrystals[J] ,” Journal of the American Chemical Society, 2018, 140(40): 12989-12995

[32] Uojun Zhou, et al. “Broad-band emission in metal halide perovskites: Mechanism, materials, and applications[J],” Materials Science & Engineering R, 2020, 141(C) : 100548-100548.

[33] Bordallo HN. et al. “Structure determination and a vibrational study for the hexagonal elpasolite Cs_2NaGaF_6 : Cr^{3+}[J],” Journal of Physics. Condensed Matter, 2002, 14(47) : 12383-12389.

[34] Sunyanming, Synthesis, “structure and properties of all inorganic cesium-containing lead-free halide double perovskites[D], ” Guilin University of Technology,2021.

[35] Gao Z, Zhang H, Mao G, et al. “Screening for lead-free inorganic double perovskites with suitable band gaps and high stability using combined machine learning and DFT calculation[J] ,” Applied Surface Science, 2021, 568: 150916.

[36] Tran T T, Panella J R, Chamorro J R, et al. “Designing indirect–direct bandgap transitions in double perovskites[J] ,” Materials Horizons, 2017, 4(4): 688-693.

[37] Iqbal S, Mustafa G M, Asghar M, et al. “Tuning the optoelectronic and thermoelectric characteristics of narrow bandgap Rb_2AlInX_6 (X= Cl, Br, I) double perovskites: A DFT study[J],”Materials Science in Semiconductor Processing, 2022, 143: 106551.

[38] Zhang L, Fang Y, Sui L, et al. “ Tuning emission and electron–phonon coupling in lead-free halide double perovskite Cs2AgBiCl6 under pressure[J],” ACS Energy Letters, 2019, 4(12): 2975-2982.

[39] Furuijing, “Structural and optical properties of inorganic diperovskite nanomaterials under high pressure[D],” Jilin University,2021.

[40] Volonakis G, Filip M R, Haghighirad A A, et al. “Lead-free halide double perovskites via heterovalent substitution of noble metals[J],” The journal of physical chemistry letters, 2016, 7(7): 1254-1259.

[41] Colella S, Mosconi E, Fedeli P, et al. “MAPbI3-xCl x mixed halide perovskite for hybrid solar cells: the role of chloride as dopant on the transport and structural properties[J],” Chemistry of Materials, 2013, 25(22): 4613-4618.

[42] Stranks S D, Eperon G E, Grancini G, et al. “Electron-hole diffusion lengths exceeding 1 micrometer in an organometal trihalide perovskite absorber[J],” Science, 2013, 342(6156): 341-344.

[43] Yangxiao, Caochenglong, Hushu et al. “Photophase separation effect in mixed halide perovskites[J],” Materials Reports,2022(16):1-27.

[44] Han D, Ogura M, Held A, et al. “Unique behavior of halide double perovskites with mixed halogens[J],” ACS Applied Materials & Interfaces, 2020, 12(33): 37100-37107.

[45] Saidaminov M I, Mohammed O F, Bakr O M, “Low-dimensional-networked metal halide perovskites: the next big thing[J],” ACS Energy Letters, 2017, 2(4): 889-896.

[46] [46]. Hu H, Meier F, Zhao D, et al. “Efficient Room - Temperature Phosphorescence from Organic–Inorganic Hybrid Perovskites by Molecular Engineering[J],” Advanced Materials, 2018, 30(36): 1707621.

[47] Kirschner M S, Diroll B T, Guo P, et al. “Photoinduced, reversible phase transitions in all-inorganic perovskite nanocrystals[J],”Nature communications, 2019, 10(1): 1-8.

[48] Zhu C, Niu X, Fu Y, et al. “Strain engineering in perovskite solar cells and its impacts on carrier dynamics[J],”Nature communications, 2019, 10(1): 1-11.